Environmental Science & Technology

Article

pubs.acs.org/est

Advanced Oxidation Kinetics and Mechanism of Preservative Propylparaben Degradation in Aqueous Suspension of TiO_2 and Risk Assessment of Its Degradation Products

Hansun Fang,[†,∥] Yanpeng Gao,[†,∥] Guiying Li,[†] Jibin An,[†,∥] Po-Keung Wong,[‡] Haiying Fu,[§] Side Yao,[§] Xiangping Nie,[⊥] and Taicheng An*[,†]

[†]State Key Laboratory of Organic Geochemistry and Guangdong Key Laboratory of Environmental Resources Utilization and Protection, Guangzhou Institute of Geochemistry, Chinese Academy of Sciences, Guangzhou 510640, China

[‡]School of Life Sciences, The Chinese University of Hong Kong, Shatin, NT, Hong Kong SAR, China

[§]Shanghai Institute of Applied Physics, Chinese Academy of Sciences, Shanghai 201800, China

[⊥]Institute of Hydrobiology, Jinan University, Guangzhou 510632, China

[∥]University of Chinese Academy of Sciences, Beijing 100049, China

Supporting Information

ABSTRACT: The absolute kinetic rate constants of propylparaben (PPB) in water with different free radicals were investigated, and it was found that both hydroxyl radicals ($HO^•$) and hydrated electrons could rapidly react with PPB. The advanced oxidation kinetics and mechanisms of PPB were investigated using photocatalytic process as a model technology, and the degradation was found to be a pseudo-first-order model. Oxidative species, particularly $HO^•$, were the most important reactive oxygen species mediating photocatalytic degradation of PPB, and PPB degradation was found to be significantly affected by pH because it was controlled by the radical reaction mechanism and was postulated to occur primarily via $HO^•$-addition or H-abstraction reactions on the basis of pulse radiolysis measurements and observed reaction products. To investigate potential risk of PPB to humans and aqueous organisms, the estrogenic assays and bioassays were performed using 100 μM PPB solution degraded by photocatalysis at specific intervals. The estrogenic activity decreased as PPB was degraded, while the acute toxicity at three trophic levels first increased slowly and then decreased rapidly as the total organic carbon decreased during photocatalytic degradation.

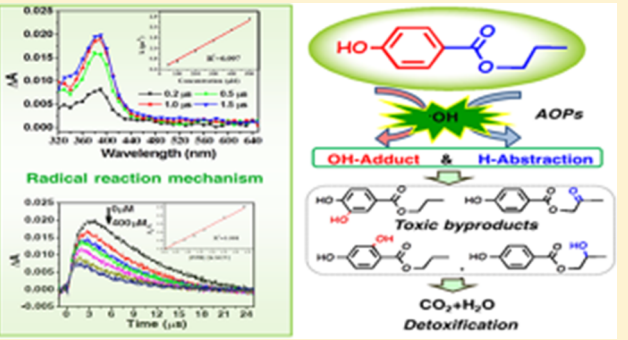

INTRODUCTION

Pharmaceutical and personal care products (PPCPs) in aquatic environments raise an emerging environmental risk, providing a new challenge to sewage and drinking water treatment systems. Parabens are important antimicrobial preservatives that are widely used in many commercial products such as cosmetics, shampoo, creams, and paper.[1,2] The persistence and increasing amount of these emerging contaminants (ECs) in surface water and sewage systems have been reported in many countries.[3−5] This has raised concern about their potential risks to aqueous organisms and humans due to their acute and chronic toxicity,[6,7] as well as estrogenic effect of propylparaben (PPB).[8,9] Parabens are listed as ECs by the U.S. Environmental Protection Agency, and toxic byproducts may form during their degradation. Thus the presence of trace amounts of parabens also may be a risk because of their combined effects with other toxic pollutants.[10] It is therefore essential to investigate the transfer and transformation characteristics, fate, and potential risk of PPB in water. The degradation kinetics, mechanism, and risk assessment of PPB by advanced oxidation processes (AOPs) to eliminate PPB from water should also be considered.

AOPs, which usually involve highly reactive hydroxyl radicals ($HO^•$), are frequently employed to remove refractory organic pollutants from water. For instance, degradation kinetics of *n*-butylparaben by H_2O_2/UV compared with direct photolysis,[11] hydroxylation mechanism of parabens by ozonation,[12] and photocatalytic kinetics of methylparaben and benzylparaben, as well as the mechanism of $HO^•$ attack, have been investigated recently.[13,14] However, the kinetics and mechanism of AOPs depend on not only the system,[15,16] but also the investigated target compounds[17] because many other active species are also involved in AOPs besides $HO^•$. That is, the degradation

Received: December 14, 2012
Revised: February 16, 2013
Accepted: February 22, 2013

   dx.doi.org/10.1021/es304898r | Environ. Sci. Technol. XXXX, XXX, XXX−XXX

mechanisms of various organics by AOPs may be different depending on the investigated method and substrate. Thus, degradation mechanisms of PPB still deserve to specify the contribution of various oxidative or reductive species produced by specific AOPs. It is at this point that pulse radiolysis provides a convenient method to trace the radical reaction process and the transient intermediates. Thus, it was usually adopted to investigate the reaction kinetics and mechanism of organic compounds with a specific radical in a complex aqueous system such as in natural water or in some AOPs systems; for example γ irradiation and photocatalytic systems.[18−20] The potential risk of transformation products and the toxicity evolution of parabens should also be considered. To date, the fate, transformation products, and toxicity evolution or the detoxification of parabens in water have not yet been attempted.

In the present study, the absolute bimolecular rate constants of PPB with hydrated electrons (e^-_{aq}) and HO$^\bullet$ are measured using pulse radiolysis to predict the redox potential of PPB in water. The advanced oxidation kinetics and mechanisms of PPB are then investigated using photocatalysis as an AOPs model. The transformation mechanisms and toxicity evolution characteristic of PPB during photocatalytic degradation are studied, and the effects of specific scavengers on the photocatalytic kinetics and mechanism are measured. Moreover, potential degradation pathways are proposed based on the identified products from both ultraperformance liquid chromatography−tandem mass spectrometry (UPLC/MS/MS) and solid-phase extraction gas chromatography−mass spectrometry (SPE-GC/MS), as well as the theoretical calculations results for free radical reactions. Finally, the estrogenic activity of PPB and its degradation products and their aqueous ecotoxicity at three different trophic levels are evaluated at different photocatalytic intervals.

EXPERIMENTAL SECTION

Materials. PPB was purchased from Tokyo Chemical Industry, Japan (99% pure), and TiO_2 nanoparticles (Degussa P25) was purchased from Degussa, Germany. All other reagents were of analytical grade and used without further purification. Luminescent bacterium (*Photobacterium phosphoreum*) was from the Institute of Soil Science, Chinese Academy of Sciences (CAS), China, *Selenastrum capricornutum* was from the Freshwater Algae Culture Collection of Institute of Hydrobiology, CAS, China, and monoclonal *Daphnia magna* was provided by Professor Xiangping Nie, Institute of Hydrobiology, Jinan University, China. All solutions were prepared using high-purity deionized water (18 MΩ cm, Millipore, USA), and solutions to investigate pulse radiation kinetics were degassed with high-purity N_2O (for HO$^\bullet$ and $^\bullet N_3$) or N_2 (for e^-_{aq}) to remove dissolved oxygen.

Pulse Radiation. Electron pulse radiolysis was performed using a 10−MeV linear accelerator (Shanghai Institute of Applied Physics, CAS, China) with a pulse length of 8 ns. Dosimetry was determined using a thiocyanate dosimeter (0.1 M KSCN saturated with N_2O) every day before experiment with an average dose of 18 Gy per pulse. A detailed description of pulse radiolysis has been presented elsewhere.[21] A Xenon lamp was used as the light source, which was passed through a quartz cell perpendicularly with electron beam. The transmitted light was collected by a monochromator equipped with a photomultiplier (R955, Hamamatsu, Japan), and the output signal was recorded by a personal computer with a digital oscillograph (LeCroy wavemaster 8600A, NY, USA). The minimum time-resolution of absorption measurements is 4 ns. The radiolysis of water is described in eq 1, where the values in parentheses indicate G values (in μmol J^{-1}).[22,23]

$$H_2O \rightarrow e^-_{aq}(0.27) + H^\bullet(0.06) + HO^\bullet(0.28) + H_2(0.05) + H_2O_2(0.07) + H_3O^+(0.27) \quad (1)$$

To study the total HO$^\bullet$ reaction kinetics with PPB, the dependence of maximum transient absorbance intensity of 120 μM potassium thiocyanate (KSCN) with different PPB concentrations was measured with a competitive kinetic equation (eq 2)[24−26]

$$\frac{Abs(SCN)_{20}^{\bullet-}}{Abs(SCN)_2^{\bullet-}} = 1 + \frac{k_T[substrate]}{k_{SCN^-}[SCN^-]} \quad (2)$$

where $Abs(SCN)_2{}^{\bullet-}{}_0$ is the maximum absorbance intensity of $(SCN)_2{}^{\bullet-}$ radical measured with pure SCN^- solution, $Abs(SCN)_2{}^{\bullet-}$ is the reduced yield of this transient radical when substrate such as PPB is added, k_T is the total bimolecular rate constant for a specific substrate reacted with HO$^\bullet$, and k_{SCN^-} is the rate constant of HO$^\bullet$ reacted with SCN^- (1.05×10^{10} M^{-1} s^{-1}).[27] A linear relationship was observed between the ratio of $Abs(SCN)_2{}^{\bullet-}{}_0/Abs(SCN)_2{}^{\bullet-}$ and that of [substrate]/[SCN^-], giving a slope of k_T/k_{SCN^-}, from which the rate constant, k_T, is obtained.

Photocatalytic Degradation and Analysis Method. Photocatalytic degradation of PPB was conducted using a constantly stirred slurry of particular TiO_2, performed in a Pyrex reactor[17] with a high-pressure mercury lamp (125 W, maximum emission at 365 nm) as a light source. The procedure is described in detail in the Supporting Information (SI). PPB concentration was measured by high-performance liquid chromatography (HPLC, Agilent 1200, Agilent, CA, USA). Total organic carbon (TOC) removal was measured with triplicates using a TOC analyzer (Shimadzu TOC-5000, Shimadzu, Japan). Both UPLC/MS/MS (Waters Xevo TQ, Micromass MS Technologies, UK) and SPE-GC/MS (Agilent 7890 GC connected to Agilent 5975 Series MSD, USA) were used to identify degradation products. Details of the analysis procedure are provided in the SI.

Computational Method. Calculations were performed with Gaussian 03.[28] The geometries and frequencies of stationary points were determined using the B3LYP/6-31G(d,p) basis set. Vibrational frequencies were calculated to ensure the stationary points were true energy minima. Time-dependent density functional theory (TD-DFT) at the B3LYP/6-311++G(d,p) level was used to calculate energies and intensities of transitions,[29] which were transformed into simulated UV/vis spectra with SWizard.[30,31]

Estrogenic Activity and Ecotoxicity Assessment. The initial concentration of 100 μM PPB was used to estimate the acute toxicity of PPB and its products during the photocatalytic degradation, and the estrogenic activity during PPB degradation was investigated with an estrogenic activity assay kit (purchased from Research Center for Eco-Environmental Sciences, CAS, China) by measuring the β-galactosidase activity of a recombinant yeast cell.[32] The ecotoxicity of PPB was evaluated at three different trophic levels: *P. phosphoreum*, *S. capricornutum*, and *D. magna*. In three sets of experiments, 2.0, 27.0, and 44.0 mL of degradation solution or pure water (control) were used, and results were normalized against the

control as percentages. *P. phosphoreum* bioassays were conducted after 15 min exposure to degradation solution with a toxicity analyzer (Dxy-3, Nanjing Kuake, China), and *S. capricornutum* bioassay was assessed by monitoring algae growth in vitro after different exposure times with a fluorometer (TD-700, Turner Designs, CA, USA).[33,34] For the toxicity bioassay with *D. magna*, each sample contained 10 individuals, and each assay was performed in triplicate. Mobilization was evaluated after 24 and 48 h of exposure to an experimental medium containing 220 mg L^{-1} $CaCl_2$, 60 mg L^{-1} $MgSO_4$, 65 mg L^{-1} $NaHCO_3$, and 6 mg L^{-1} KCl. The estimation program interface (EPI) suite was used to estimate LC_{50} values (the concentration that kills half the members of tested organisms after a specified test duration) of *D. magna* exposed for 48 h, and EC_{50} values (the concentration that presented 50% of the compound's maximal effect on the tested organisms after a specified test duration) of algae after 96 h.

RESULTS AND DISCUSSION

HO• and e^-_{aq}–Mediated Degradation Kinetics and Mechanism of PPB. Pulse radiolysis was employed to investigate the transformation characteristics and fate of ECs in water as well as the use of advanced oxidation/reduction to degrade ECs in water. Pulse radiolysis can supply transient reaction and absolute reaction rate constants of PPB with both HO• and e^-_{aq}. The solution was presaturated with N_2O, which can quantitatively convert e^-_{aq} and H• into HO•.[20,22,27] Also, e^-_{aq} can be obtained quantitatively by presaturation with N_2 in the presence of 0.1 M *tert*-butyl alcohol (*tert*-BuOH) to convert both HO• and H• into relatively inert *tert*-BuOH radicals.[20]

Figure 1a presents time-resolved transient absorption spectra of HO• with 300 μM PPB in pure water. An intense peak at 390 nm is mainly ascribed to the absorption of an HO•-adduct, along with a small shoulder at 330 nm. The transient species was stable for 1.5 μs and then decreased rapidly. The bimolecular rate constant of PPB with HO• was calculated to be 4.65 ± 0.23 × 10^9 M^{-1} s^{-1} from the slope of the curve by plotting pseudo-first-order growth rate constant against PPB concentration (inset of Figure 1a). Besides HO•-addition, H-abstraction and electron transfer reactions can also occur.[35] Thus, the total rate constant of PPB with HO• was also measured by a competitive method employing SCN^- in the pulse radiolysis solution.[24,36] Kinetic formation curves for $(SCN)_2^{\bullet-}$ at 480 nm with different PPB concentrations gave a bimolecular rate constant (k_T) of 7.70 ± 0.39 × 10^9 M^{-1} s^{-1} using eq 2 (Figure S1). The difference of 3.05 ± 0.15 × 10^9 M^{-1} s^{-1} between k_T and direct rate constant indicates OH-adducts were not the only intermediates formed in the reaction of PPB with HO•. To validate transient intermediates observed at 390 nm and explore immeasurable species, UV/vis spectra of PPB and its transient intermediates were conducted and compared with calculated data (Figure 2). It was found that the calculated spectra were similar to experimental ones. The measurable transient at 390 nm is obviously HO•-adduct intermediate, and the radical cation of PPB ($PPB^{\bullet+}$) with a calculated peak at 422 nm results from electron transfer with HO•. Thus the calculated transient profile of H-abstraction reaction exhibited a peak at 248 nm that would contribute to the rate constant of 3.05 ± 0.23 × 10^9 M^{-1} s^{-1} because the peak of electron transfer reaction of PPB with HO•, if formed, would rapidly transform into the HO•-addition intermediate in aqueous environment.[22] To further confirm the electron transfer between PPB and HO•, $^{\bullet}N_3$ (E^0 = 1.33 V vs NHE) was introduced as a mild oxidative radical and good electron-transfer reagent in presaturated N_2O solutions containing 50 mM NaN_3,[22] and a double peak was obviously found around 420 nm (Figure S2), which was assigned to phenoxyl radical formed by radical cation in aqueous solution.[37] A bimolecular rate constant of 6.30 ± 0.32 × 10^8 M^{-1} s^{-1} was obtained from the regression of pseudo-first-order reaction rate constants (inset of Figure S2). Both from the relatively low rate constant of electron transfer and the absence of a shoulder peak at 420 nm in the experimental spectra we can further confirm low electron-transfer reactivity of HO• to PPB. Overall, HO•-addition pathway onto aromatic ring played the most important role in initiating reaction of PPB with a rate constant of 4.65 ± 0.23 × 10^9 M^{-1} s^{-1}. H abstraction from propyl chain with a rate constant of 3.05 ± 0.15 × 10^9 M^{-1} s^{-1} had a smaller contribution, and electron transfer might be ignored because of its inconspicuous peak on transient spectra and much lower rate constant.

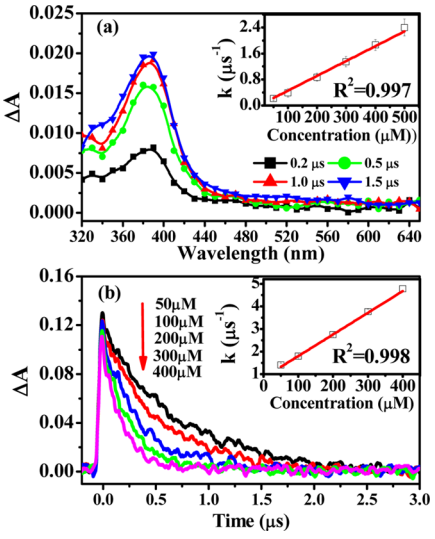

Figure 1. (a) Transient absorption spectra from the reaction of HO• radicals with 300 μM PPB in pure water saturated with N_2O at different time intervals. The inset shows a plot of pseudo-first-order transient formation rate constants at 390 nm vs. PPB concentration. (b) Typical decay kinetics of e^-_{aq} of solutions containing different concentrations of PPB, 0.1 M *tert*-BuOH, and saturated with N_2. The inset contains a plot of pseudo-first-order transient reaction rate constants vs. PPB concentration.

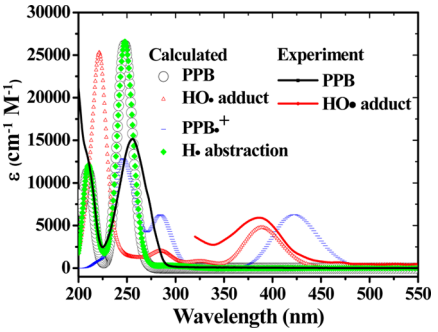

Figure 2. (a) Experimental and (b) calculated UV/vis absorption spectra of PPB and transient intermediates.

dx.doi.org/10.1021/es304898r | Environ. Sci. Technol. XXXX, XXX, XXX–XXX

As a phenolic compound with pK_a value of 8.24, PPB mainly existed as a neutral molecule at low pH value under pK_a, while it mainly existed as a negative species when pH value was higher than pK_a. Thus, the reaction of PPB with HO$^\bullet$ was expected to be significantly affected by pH value because pH may determine radical reaction mechanisms of HO$^\bullet$ with PPB. Figure 3 shows a peak at 390 nm in neutral solution and then

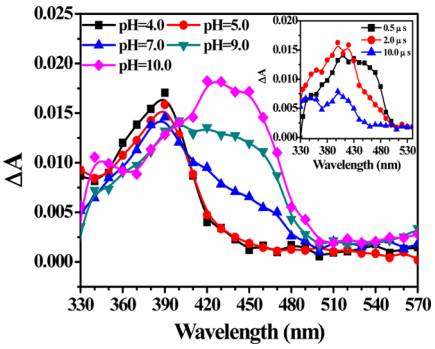

Figure 3. Transient absorption spectra of 300 μM PPB reacted with HO$^\bullet$ radicals in N_2O-saturated solution at different pH. The inset shows absorption spectra measured at different time intervals at pH 9.0.

gradually shifted to 420−450 nm due to HO$^\bullet$ adduct reaction with PPB anion. Results show that phenoxyl radical presents almost no peak around 420 nm at acidic and in pure water, and formed a strong peak rapidly within 2.0 μs at pH = 9.0 (inset of Figure 3). That is, at acidic condition, PPB reacts with HO$^\bullet$ to form a clear peak of HO$^\bullet$-adduct, while alkaline conditions could facilitate the formation of phenoxyl radical by catalytic effect. Similar results were also obtained with phenol.[38]

To further confirm the reaction of PPB with e^-_{aq}, transient reaction(s) and absolute reaction rate constants were also investigated. However, except for the wide absorption band of 380 to 700 nm of e^-_{aq}, no significant transient was observed (data not shown). Therefore, the kinetic decay profiles for e^-_{aq} reacting with different PPB concentrations were measured (Figure 1b). By fitting pseudo-first-order exponential decay kinetics at different values of [PPB], the second-order rate constant was calculated (inset of Figure 1b). The slope gave a rate constant of $9.71 \pm 0.48 \times 10^9$ M^{-1} s^{-1} for the reaction of PPB with e^-_{aq}. This rate constant is slightly higher than that of HO$^\bullet$, indicating that e^-_{aq} could also be involved in photochemical transformation of PPB, and the advanced reduction by e^-_{aq} might also be an important pathway for PPB degradation in environmental water.

Photocatalytic Degradation Kinetics of PPB. Photocatalysis was employed to study advanced oxidation of PPB and probe its fate in water. Degradation kinetics was optimized with respect to TiO_2 dosage, PPB concentration, and pH value, and results showed that PPB degradation followed pseudo-first-order kinetics at various conditions. The pseudo-first-order rate constant (k_1) increased slowly with increasing TiO_2 dosage from 0.5 to 4.0 g L^{-1}, and decreased gradually with increasing PPB concentration from 20 to 200 μM (Figure S3). For pH value, k_1 decreased slightly with increasing pH from 3.0 to 9.0 and then decreased rapidly at pH 11.0. The change trend of k_1 at different pH values can be well explained from the point of view of the above-mentioned radical-involved mechanism. Furthermore, detailed kinetic optimization and an explanation of the effect of pH on k_1 also related to adsorption capability (Figure S4) as presented in SI. The half-life of PPB in photocatalytic process is 3.5−76.2 min at investigated conditions, while direct photolysis of PPB is almost negligible with a half-life of 3465.7 min (Table S1). This implies PPB could be easily degraded by AOPs, but not so easily degraded by direct photolysis.

Considering reactive species such as photogenerated holes (h^+) and HO$^\bullet_{ads}$ only functioned near or on the surface of TiO_2, it is unsurprising that higher degradation rate constants were obtained in acidic solution due to relatively higher absorption coefficients of PPB (Figure S5 and Table S1). The direct electron transfer from the adsorbed PPB to valence band provided a potential way to form radical cation of PPB, which would transform into HO$^\bullet$-adduct finally. However, rate constants did not depend directly on the adsorption of PPB onto TiO_2. As mentioned, alkaline conditions could dramatically enhance the formation of phenoxyl radical of PPB, which can react with e^-_{aq} to regenerate the parent compound,[39] decreasing PPB degradation rate in strongly alkaline solution. Furthermore, HO$^\bullet$ (pK_a = 11.9) can also transform into less reactive oxide radical ion ($O^{\bullet-}$) and thus result in the decrease of degradation rate constant at high pH value.[27]

Contributions of Different Reactive Species. In photocatalysis, a series of oxidative or reductive species, such as h^+ and e^-_{aq}, as well as resulted HO$^\bullet$, $O_2^{\bullet-}$, and H_2O_2, are produced (Figure S6) that can react with various ECs. The bimolecular rate constants obtained above suggested that both oxidative (HO$^\bullet$) and reductive species (e^-_{aq}) could rapidly react with PPB, but the contribution from each species is still unclear in AOPs degradation of PPB. Therefore, the photocatalytic degradation kinetics of PPB with or without specific scavengers (Table S2) was conducted: 0.1 M isopropanol was used to scavenge HO$^\bullet$,[17] 0.1 M methanol was used to remove the contribution of h^+ and HO$^\bullet$,[40] 0.1 M KI was used to remove h^+ and surface HO$^\bullet_{ads}$,[41] 0.1 mM NaF was used to wash HO$^\bullet_{abs}$ into solution as bulk HO$^\bullet_{bulk}$,[42] 50 μM $K_2Cr_2O_7$ was used to remove e^-_{aq} in solution,[43] and MeCN was used to rule out the participation of HO$^\bullet$.[44,45] The degradation kinetics is depicted in Figure 4, and the variation of pseudo-first-order rate constants under different conditions is also summarized in Table S2. The rate constant was 0.0272 min^{-1} in photocatalytic system without any scavengers, but it decreased to 0.0042 min^{-1} when HO$^\bullet$ was removed by isopropanol, indicating HO$^\bullet$ contribution to PPB degradation of 84.6%. With methanol addition, the rate constant decreased notably to 0.0023 min^{-1}, suggesting 91.5% of the rate originated from both HO$^\bullet$ and h^+. This result indicates that h^+ also engaged in photocatalytic degradation of PPB probably by direct electron transfer process, but the reaction only contributed to 6.9%. The rate constant reduced to 0.0080 min^{-1} (by 70.6%) in the presence of KI, suggesting that PPB degradation was mostly induced by HO$^\bullet_{ads}$. The rate constant was obtained as 0.0514 min^{-1} in presence of NaF, increasing by 89.0%. This may be caused by enhanced transformation of HO$^\bullet_{ads}$ to HO$^\bullet_{bulk}$ for PPB oxidation. The rate constant in MeCN reached 0.0188 min^{-1} when PPB adsorption efficiency was as high as 19.3% within 30 min (data not shown), suggesting high reactivity of h^+ with adsorbed PPB.

Interestingly, quenching e^-_{aq} produced at TiO_2 conduction band under UV irradiation by adding $K_2Cr_2O_7$ decreased the rate constant to 0.0056 min^{-1} by 79.4%. The weak light screen effect by 50 μM $K_2Cr_2O_7$ would probably not result in this dramatic decrease. To eliminate the interference of light

dx.doi.org/10.1021/es304898r | Environ. Sci. Technol. XXXX, XXX, XXX−XXX

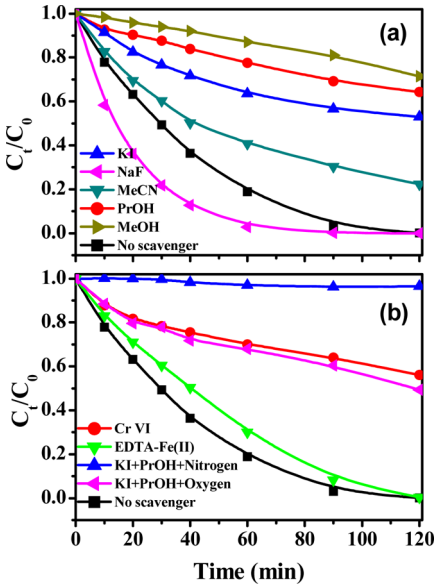

Figure 4. Photocatalytic degradation kinetics of 100 μM PPB and 2.0 g L^{-1} TiO_2 in the presence of various scavengers: 0.1 M isopropanol, 0.1 M methanol, 0.1 M KI, 50 μM $K_2Cr_2O_7$, 10 μM Fe(II)-EDTA, 0.1 M KI + 0.1 M isopropanol + N_2, 0.1 M KI + 0.1 M isopropanol + O_2, and in pure acetonitrile.

absorption of scavengers and further understand the roles of conduction band species, three more experiments were performed (Figure 4b and Table S2). A solution containing 0.1 M KI and 0.1 M isopropanol degassed with N_2 was used to exclude all other species except reductive e^-_{aq},[15] and the rate constant was obtained as 0.0004 min^{-1} in this solution, indicating that e^-_{aq} only contributed to 1.5% degradation rate, even though e^-_{aq} reacted with PPB with a high rate constant. This difference may imply other species were formed from e^-_{aq} to help PPB degradation. To confirm this assumption, PPB degradation was also conducted in presence of 0.1 M KI, 0.1 M isopropanol, and O_2 to transform e^-_{aq} into relative oxidative species.[46] A rate constant of 0.0089 min^{-1} was observed, indicating $O_2^{-\bullet}$ contributed to 32.7% PPB degradation, and the remainder was from other oxidative species produced from e^-_{aq} such as H_2O_2. The indirect contribution from e^-_{aq} was further confirmed when 10 μM Fe(II)-EDTA was used to quench H_2O_2, which caused rate constant decrease to 0.0195 min^{-1} by 28.3%.[15,47]

Overall, oxidative species, in particular $HO^\bullet$, formed at TiO_2 valence band were predominantly responsible for PPB degradation in water, and h^+ was not remarkable due to low adsorptive capacity of PPB in aqueous although h^+ had high reactivity to PPB. A smaller contribution was associated with indirect degradation of reductive species e^-_{aq} which produced various oxidative species at TiO_2 conduction band.

Photocatalytic Degradation Mechanism of PPB. Both UPLC/MS/MS and SPE/GC/MS were used to separate and identify products formed during photocatalytic degradation of PPB. Eleven products were identified by UPLC/MS/MS and six were confirmed by SPE/GC/MS through their retention times (t_R), and structural assignment based on analysis of both molecular ion peaks and cleavage patterns. Total ion current (TIC) chromatograms from UPLC/MS/MS and SPE/GC/MS

Scheme 1. Proposed Photocatalytic Degradation Pathways and Mechanism of PPB in Water

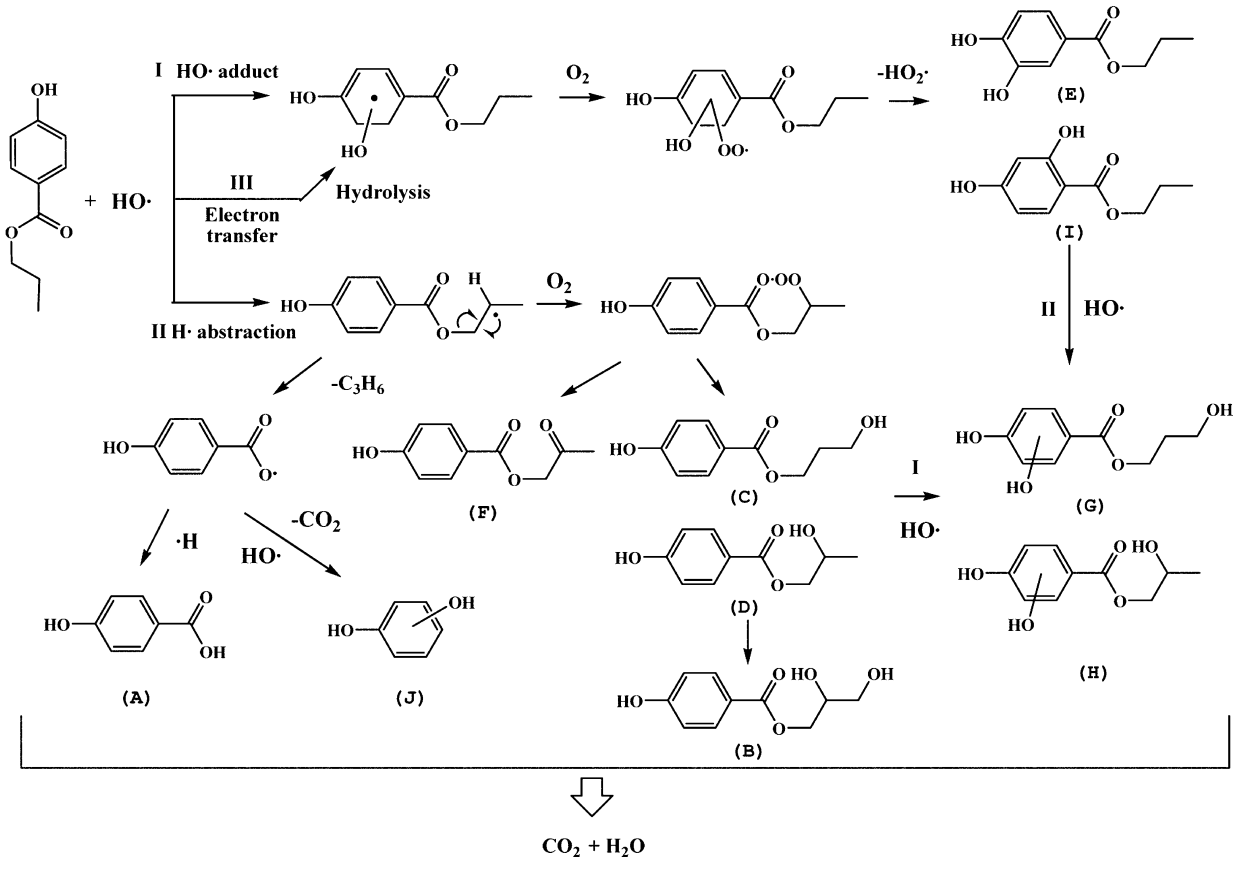

dx.doi.org/10.1021/es304898r | Environ. Sci. Technol. XXXX, XXX, XXX–XXX

are shown in Figures S7 and S8, respectively. The structure and relative parameters of proposed products are summarized in Table S3. The fragmentation patterns of each product are also illustrated in Figures S9 and S10, and identification and assignment of each product are also presented in the SI.

In UPLC/MS/MS TIC chromatograms, the t_R values of all products were shorter than that of PPB, indicating that they were more hydrophilic than PPB. Four products (C, D, E, and I) with m/z 195 were obtained, corresponding to the addition of 16 mass units to PPB (m/z 179), consistent with PPB monohydroxylated products. Simultaneously, three products with m/z 211 (B, G, and H) were also detected, corresponding to dihydroxylated derivatives of PPB. Another product with m/z 193 (F) was identified as the compound with a carbonyl group replacing with a hydroxyl group on alkyl chain of 2-hydroxy-propyl, 4-hydroxybenzoate (m/z 195). A product with m/z 137 was identified as 4-hydroxybenzoic acid (A), which was also validated by both its t_R (0.97 min) and fragmentation pattern of an authentic standard (Figure S11). Two other products with m/z 97 (t_R = 0.79 min) and 165 (t_R = 3.00 min) were also detected by UPLC/MS/MS, for which we were unable to assign structures. Products D, E, F, and I were further confirmed by their fragmentation patterns in SPE/GC/MS (Figure S10), and two additional products (J and K) with m/z 110 were assigned to dihydroxybenzene because their fragmentation patterns were similar to that of dihydroxybenzene in the NIST database.

The above results indicated HO$^\bullet$ was the largest contributor in the photocatalytic degradation of PPB, and several products were found to be hydroxylated via either the aromatic ring or propyl ester chain mainly through an HO$^\bullet$-adduct or H abstraction. Combining all information, three predominant degradation pathways were proposed for HO$^\bullet$ initiating attack to PPB (Scheme 1). In pathways 1 and 3, HO$^\bullet$ reacts with PPB to form an HO$^\bullet$-adduct, producing a series of hydroxylated products on aromatic rings, such as 2-hydroxypropyl paraben (E) and 3-hydroxypropyl paraben (I). In pathway 2, HO$^\bullet$ attacks PPB through H abstraction, and the resulting carbon-centered radical reacts with oxygen dissolved in water to form a peroxy radical. This peroxy intermediate primarily formed a tetroxide, which could decompose into hydroxyl and carbonyl groups on the alkyl chain through the Russell or Bennett reaction mechanism,[48−52] producing products such as 2-hydroxypropyl, 4-hydroxybenzoate (B) and 2-ketonepropyl, 4-hydroxybenzoate (F). The dihydroxylated products with m/z 211 were produced by further hydroxylation of monohydroxylated products (m/z 195, C, D, E and I), where the aromatic ring and ester chain form hydroxylated products such as 2-hydroxypropyl dihydroxybenzoate (H). 4-Hydroxybenzoic acid (A) could be formed in pathway 2 by losing one molecule of propylene. Of course, by prolonging the degradation time, these hydroxylated products could be further decomposed into other low-molecular-weight products such as dihydroxybenzene (J).

Estrogenic Activity and Ecotoxicity Evolution of PPB Solutions. To investigate the potential risk of PPB as well as its degradation products to human health, the estrogenic activity evolution of during PPB degradation was evaluated (Figure 5a). The EC_{50} value of 17-β-estradiol was first determined as 1.5 ± 0.2 × 10^{-10} M by fitting the sigmoidal dose−response curve (Figure S12) which is comparable with the referred data of yeast estrogen screen assay (4.4 ± 1.5 × 10^{-10} M),[53] validating the performance of this estrogenic

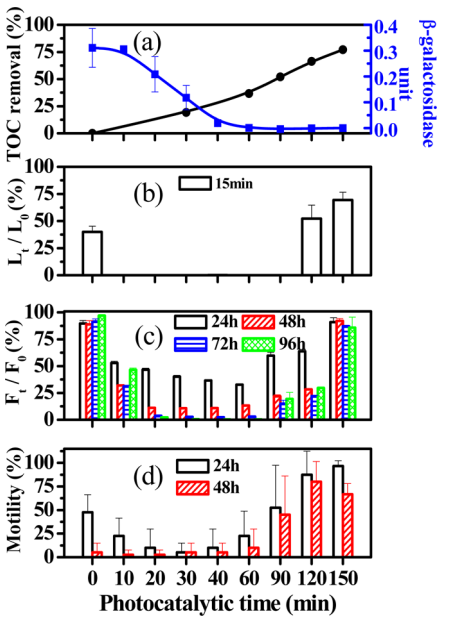

Figure 5. (a) Evolution of both TOC removal efficiencies (black curve, left y-axis) and estrogenic activity (blue curve, right y-axis), and acute toxicity evaluated with (b) *Photobacterium phosphoreum*, (c) *Selenastrum capricornutum*, and (d) *Daphnia magna* during the photocatalytic degradation of 100 μM PPB by 2.0 g L^{-1} TiO_2.

activity assay. The estrogenic activity of degraded PPB solution decreased rapidly from 0 to 60 min, and then decreased to below detection limits within 90 min as the TOC removal efficiency increased. The constant decrease implies that the estrogenic activity of degraded solution is related to PPB rather than degradation products, indicating that the estrogenic activity of products during photocatalytic degradation can be ignored.

To further understand the fate and potential risk of PPB in water treated by AOPs, the ecotoxicity evolution was evaluated during photocatalytic degradation at three different trophic levels, *P. phosphoreum*, *S. capricornutum*, and *D. magna* (Figure 5b−d). *P. phosphoreum*, *S. capricornutum* (96 h exposure), and *D. magna* (48 h exposure) were inhibited by 39.9%, 96.8%, and 5.0%, respectively. As degradation progressed, the inhibition efficiencies increased and the ecotoxicity of treated solution toward three species all increased with the increase of degradation time. The luminescence of *P. phosphoreum* decreased completely from 10 to 90 min, and the fluorescence of *S. capricornutum* decreased constantly until 40 min. The PPB solution treated for 30 min was the most toxic sample to *D. magna*. That is, the toxicity toward three aqueous organisms increased initially and then decreased as TOC reduced, suggesting that products may possess higher toxicity than PPB to these three aqueous organisms during degradation. This increased toxicity might be caused by the formation of phenolic products with high hydroxylation, and similar results were obtained previously.[54,55]

From the above, PPB degradation mainly initiated by HO$^\bullet$ either through HO$^\bullet$-adduct or H abstraction. To primarily examine the contribution of each pathway to total toxicity, the LC_{50} and EC_{50} values of each product were calculated using EPI suite (Table S3). Products (C, D, and F) formed by H-abstraction possess LC_{50} from 19.345 to 21.389 mg L^{-1}, and products (E and I) from HO$^\bullet$-adduct present LC_{50} from 11.646 to 107.363 mg L^{-1}. However, EC_{50} values of the products

dx.doi.org/10.1021/es304898r | Environ. Sci. Technol. XXXX, XXX, XXX−XXX

resulted from H-abstraction pathway of 93.277−103.988 mg L^{-1} were much higher than those from the $HO^{\bullet}$-adduct pathway (1.332−1.721 mg L^{-1}). These results indicate the products from $HO^{\bullet}$-adduct pathway possess higher toxicity than those from the H-abstraction pathway. Thus we can conclude that the toxicity was predominantly from intermediates hydroxylated on the aromatic ring from $HO^{\bullet}$-adduct pathway. Degradation of PPB and its products with sufficient period would decrease TOC and detoxify PPB solution because more harmful products were further decomposed and transformed to CO_2 and H_2O. That is, the initial increased acute toxicity observed during PPB degradation implies the treatment time of AOPs should be determined carefully for safe water treatment.

Fate Prediction of Similar ECs. The obtained results about initial reaction and reaction pathways in AOPs could be used to tentatively predict the fate of other ECs with a structure similar to PPB. The degradation of specific ECs both with an aromatic ring and alkyl chain is always initiated by $HO^{\bullet}$ through both $HO^{\bullet}$-addition and H-abstraction mechanism. That is, the former reaction always occurs onto aromatic ring, while the latter reaction always happens to alkyl chain. To validate this assumption, the transient reaction kinetics of ethylparaben and 4-hydroxybenzoic acid (HB) with $HO^{\bullet}$ were also studied by pulse radiolysis (Figure S13a−d). The bimolecular rate constants of $HO^{\bullet}$-adduct transient (k_A) were obtained by measuring the growth kinetics at 390 or 380 nm. The competitive method was used to measure the total bimolecular rate constant (k_T), and the difference between these two rate constants gives the H-abstraction rate constant, k_H. The values of k_A, k_H, and k_T for PPB, ethylparaben, and HB are summarized in Table S4. It was found that k_H increased with increasing alkyl chain, from $<0.69 \times 10^9$ M^{-1} s^{-1} for HB to $3.05 \pm 0.15 \times 10^9$ M^{-1} s^{-1} for PPB. Furthermore, the rate of both initial reactions may determine the composition of degradation byproducts, which subsequently resulted in transformation patterns of ECs, such as the fate and toxicity. The above-obtained results for PPB suggest that degradation products with higher toxicity than PPB would form primarily through $HO^{\bullet}$-adduct in the advanced oxidation of these ECs with a short alkyl chain. That is, ECs with a long alkyl chain on aromatic ring would be decomposed mainly through H abstraction resulting in primary byproducts with lower toxicity. The results suggest the transformation mechanism and the fates of these ECs in water are depending on not only AOPs system but also ECs structure. Of course, the results will gain in-depth understanding on the free radical reaction kinetics and mechanism of PPB and other ECs with similar structures.

■ ASSOCIATED CONTENT

Supporting Information

Detailed descriptions of experiments and analysis of photocatalytic degradation products. This material is available free of charge via the Internet at http://pubs.acs.org.

■ AUTHOR INFORMATION

Corresponding Author

*Tel: +86-20-85291501; fax: +86-20-85290706; e-mail: antc99@gig.ac.cn.

Notes

The authors declare no competing financial interest.

■ ACKNOWLEDGMENTS

This contribution is No. 1609 from GIGCAS. Pulse radiolysis research was undertaken at the Shanghai Institute of Applied Physics, CAS. Dr. Weizhen Lin is thanked for help and useful discussion. This work was financially supported by the Knowledge Innovation Program of CAS (KZCX2-YW-QN103), NSFC (40973068), the Earmarked Fund of the SKLOG (SKLOG2012A01), and the Science and Technology R&D Fund of Shenzhen City (JC201005250054A).

■ REFERENCES

(1) Vinggaard, A. M.; Korner, W.; Lund, K. H.; Bolz, U.; Petersen, J. H. Identification and quantification of estrogenic compounds in recycled and virgin paper for household use as determined by an in vitro yeast estrogen screen and chemical analysis. *Chem. Res. Toxicol.* **2000**, *13* (12), 1214−1222, DOI: 10.1021/tx000146b.

(2) Rudel, R. A.; Perovich, L. J. Endocrine disrupting chemicals in indoor and outdoor air. *Atmos. Environ.* **2009**, *43* (1), 170−181, DOI: 10.1016/j.atmosenv.2008.09.025.

(3) Peng, X. Z.; Yu, Y. J.; Tang, C. M.; Tan, J. H.; Huang, Q. X.; Wang, Z. D. Occurrence of steroid estrogens, endocrine-disrupting phenols, and acid pharmaceutical residues in urban riverine water of the Pearl River Delta, South China. *Sci. Total Environ.* **2008**, *397* (1−3), 158−166, DOI: 10.1016/j.scitotenv.2008.02.059.

(4) Jonkers, N.; Kohler, H. P. E.; Dammshauser, A.; Giger, W. Mass flows of endocrine disruptors in the Glatt River during varying weather conditions. *Environ. Pollut.* **2009**, *157* (3), 714−723, DOI: 10.1016/j.envpol.2008.11.029.

(5) Regueiro, J.; Llompart, M.; Psillakis, E.; Garcia-Monteagudo, J. C.; Garcia-Jares, C. Ultrasound-assisted emulsification-microextraction of phenolic preservatives in water. *Talanta* **2009**, *79* (5), 1387−1397, DOI: 10.1016/j.talanta.2009.06.015.

(6) Yamamoto, H.; Tamura, I.; Hirata, Y.; Kato, J.; Kagota, K.; Katsuki, S.; Yamamoto, A.; Kagami, Y.; Tatarazako, N. Aquatic toxicity and ecological risk assessment of seven parabens: Individual and additive approach. *Sci. Total Environ.* **2011**, *410*, 102−111, DOI: 10.1016/j.scitotenv.2011.09.040.

(7) Terasaki, M.; Makino, M.; Tatarazako, N. Acute toxicity of parabens and their chlorinated by-products with *Daphnia magna* and *Vibrio fischeri* bioassays. *J. Appl. Toxicol.* **2009**, *29* (3), 242−247, DOI: 10.1002/jat.1402.

(8) Pugazhendhi, D.; Pope, G. S.; Darbre, P. D. Oestrogenic activity of p-hydroxybenzoic acid (common metabolite of paraben esters) and methylparaben in human breast cancer cell lines. *J. Appl. Toxicol.* **2005**, *25* (4), 301−309, DOI: 10.1002/jat.1066.

(9) Terasaka, S.; Inoue, A.; Tanji, M.; Kiyama, R. Expression profiling of estrogen-responsive genes in breast cancer cells treated with alkylphenols, chlorinated phenols, parabens, or bis- and benzoylphenols for evaluation of estrogenic activity. *Toxicol. Lett.* **2006**, *163* (2), 130−141, DOI: 10.1016/j.toxlet.2005.10.005.

(10) Kim, Y. R.; Jung, E. M.; Choi, K. C.; Jeung, E. B. Synergistic effects of octylphenol and isobutyl paraben on the expression of calbindin-D(9k) in GH3 rat pituitary cells. *Int. J. Mol. Med.* **2012**, *29* (2), 294−302, DOI: 10.3892/ijmm.2011.823.

(11) Bledzka, D.; Gmurek, M.; Gryglik, M.; Olak, M.; Miller, J. S.; Ledakowicz, S. Photodegradation and advanced oxidation of endocrine disruptors in aqueous solutions. *Catal. Today* **2010**, *151* (1−2), 125−130, DOI: 10.1016/j.cattod.2010.03.040.

(12) Tay, K. S.; Rahman, N. A.; Bin Abas, M. R. Ozonation of parabens in aqueous solution: Kinetics and mechanism of degradation. *Chemosphere* **2010**, *81* (11), 1446−1453, DOI: 10.1016/j.chemosphere.2010.09.004.

(13) Lin, Y. X.; Ferronato, C.; Deng, N. S.; Chovelon, J. M. Study of benzylparaben photocatalytic degradation by TiO_2. *Appl. Catal., B* **2011**, *104* (3−4), 353−360, DOI: 10.1016/j.apcatb.2011.03.006.

(14) Lin, Y. X.; Ferronato, C.; Deng, N. S.; Wu, F.; Chovelon, J. M. Photocatalytic degradation of methylparaben by TiO_2: Multivariable

experimental design and mechanism. *Appl. Catal., B* **2009**, *88* (1−2), 32−41, DOI: 10.1016/j.apcatb.2008.09.026.

(15) Chen, Y. M.; Lu, A. H.; Li, Y.; Zhang, L. S.; Yip, H. Y.; Zhao, H. J.; An, T. C.; Wong, P. K. Naturally occurring sphalerite as a novel cost-effective photocatalyst for bacterial disinfection under visible light. *Environ. Sci. Technol.* **2011**, *45* (13), 5689−5695, DOI: 10.1021/es200778p.

(16) Wang, W. J.; Yu, Y.; An, T. C.; Li, G. Y.; Yip, H. Y.; Yu, J. C.; Wong, P. K. Visible-light-driven photocatalytic inactivation of *E. coli* K-12 by bismuth vanadate nanotubes: Bactericidal performance and mechanism. *Environ. Sci. Technol.* **2012**, *46* (8), 4599−4606, DOI: 10.1021/es2042977.

(17) Yang, H.; An, T. C.; Li, G. Y.; Song, W. H.; Cooper, W. J.; Luo, H. Y.; Guo, X. D. Photocatalytic degradation kinetics and mechanism of environmental pharmaceuticals in aqueous suspension of TiO_2: A case of beta-blockers. *J. Hazard. Mater.* **2010**, *179* (1−3), 834−839, DOI: 10.1016/j.jhazmat.2010.03.079.

(18) Razavi, B.; Ben Abdelmelek, S.; Song, W.; O'Shea, K. E.; Cooper, W. J. Photochemical fate of atorvastatin (lipitor) in simulated natural waters. *Water Res.* **2011**, *45* (2), 625−631, DOI: 10.1016/j.watres.2010.08.012.

(19) Song, W. H.; Cooper, W. J.; Mezyk, S. P.; Greaves, J.; Peake, B. M. Free radical destruction of beta-blockers in aqueous solution. *Environ. Sci. Technol.* **2008**, *42* (4), 1256−1261, DOI: 10.1021/es702245n.

(20) An, T. C.; Yang, H.; Song, W. H.; Li, G. Y.; Luo, H. Y.; Cooper, W. J. Mechanistic considerations for the advanced oxidation treatment of fluoroquinolone pharmaceutical compounds using TiO_2 heterogeneous catalysis. *J. Phys. Chem. A* **2010**, *114* (7), 2569−2575, DOI: 10.1021/jp911349y.

(21) Hou, H. Q.; Luo, C.; Liu, Z. X.; Mao, D. M.; Qin, Q. Z.; Lian, Z. R.; Yao, S. D.; Wang, W. F.; Zhang, J. S.; Lin, N. Y. Generation of the C-60 radical cation via electron-transfer reaction - A pulse-radiolysis study. *Chem. Phys. Lett.* **1993**, *203* (5−6), 555−559, DOI: 10.1016/0009-2614(93)85309-C.

(22) Nicolaescu, A. R.; Wiest, O.; Kamat, P. V. Radical-induced oxidative transformation of quinoline. *J. Phys. Chem. A* **2003**, *107* (3), 427−433, DOI: 10.1021/jp027112s.

(23) An, T. C.; Yang, H.; Li, G. Y.; Song, W. H.; Cooper, W. J.; Nie, X. P. Kinetics and mechanism of advanced oxidation processes (AOPs) in degradation of ciprofloxacin in water. *Appl. Catal., B* **2010**, *94* (3−4), 288−294, DOI: 10.1016/j.apcatb.2009.12.002.

(24) McKay, G.; Dong, M. M.; Kleinman, J. L.; Mezyk, S. P.; Rosario-Ortiz, F. L. Temperature Dependence of the Reaction between the Hydroxyl Radical and Organic Matter. *Environ. Sci. Technol.* **2011**, *45* (16), 6932−6937, DOI: 10.1021/es201363j.

(25) Peller, J.; Wiest, O.; Kamat, P. V. Hydroxyl radical's role in the remediation of a common herbicide, 2,4-dichlorophenoxyacetic acid (2,4-D). *J. Phys. Chem. A* **2004**, *108* (50), 10925−10933, DOI: 10.1021/jp0464501.

(26) Song, W.; Yan, S.; Cooper, W. J.; Dionysiou, D. D.; O'shea, K. E. Hydroxyl radical oxidation of cylindrospermopsin (cyanobacterial Toxin) and its role in the photochemical transformation. *Environ. Sci. Technol.* **2012**, *46* (22), 12608−12615, DOI: 10.1021/es302458h.

(27) Buxton, G. V.; Greenstock, C. L.; Helman, W. P.; Ross, A. B. Critical-review of rate constants for reactions of hydrated electrons, hydrogen-atoms and yydroxyl radicals ($\cdot OH/\cdot O^-$) in aqueous-solution. *J. Phys. Chem. Ref. Data* **1988**, *17* (2), 513−886, DOI: 10.1063/1.555805.

(28) Frisch, M. J.; Truck, G. W.; Schlegel, H. B.; Scuseria, G. E.; Robb, M. A.; Cheeseman, J. R.; Zakrzewski, V. G.; Montgomery, J. A.; Stratmann, J. R. E.; Burant, J. C.; Dapprich, S.; Millam, J. M.; Daniels, A. D.; Kudin, K. N.; Strain, M. C.; Farkas, O.; Tomasi, J.; Barone, V.; Cossi, M.; Cammi, R.; Mennucci, B.; Pomelli, C.; Adamo, C.; Clifford, S.; Ochterski, J.; Petersson, G. A.; Ayala, P. Y.; Cui, Q.; Morokuma, K.; Malick, D. K.; Rabuck, A. D.; Raghavachari, K.; Foresman, J. B.; Cioslowski, J.; Ortiz, J. V.; Boboul, A. G.; Stefnov, B. B.; Liu, G.; Liaschenko, A.; Piskorz, P.; Komaromi, L.; Gomperts, R.; Martin, R. L.; Fox, D. J.; Keith, T.; Al−Laham, M. A.; Peng, C. Y.; Nanayakkara, A.; Gonzalez, C.; Challacombe, M.; Gill, P. M. W.; Johnson, B.; Chen, W.; Wong, M. W.; Andres, J. L.; Gonzalez, C.; Head−Gordon, M.; Replogle, E. S.; Pople, J. A. *GAUSSIAN 03, Revision A.1*; Guassian, Inc.: Pittsburgh, PA, 2003.

(29) Galano, A.; Alvarez-Idaboy, J. R. Guanosine plus OH radical reaction in aqueous solution: A reinterpretation of the UV-vis data based on thermodynamic and kinetic calculations. *Org. Lett.* **2009**, *11* (22), 5114−5117, DOI: 10.1021/ol901862h.

(30) Gorelsky, S. I. *SWizard program*, http://www.sg-chem.net/; University of Ottawa: Canada, 2010.

(31) Gorelsky, S. I.; Lever, A. B. P. Electronic structure and spectral, of ruthenium diimine complexes by density functional theory and INDO/S. Comparison of the two methods. *J. Organomet. Chem.* **2001**, *635* (1−2), 187−196, DOI: 10.1016/S0022-328X(01)01079-8.

(32) Li, G. Y.; Zu, L.; Wong, P. K.; Hui, X. P.; Lu, Y.; Xiong, J. K.; An, T. C. Biodegradation and detoxification of bisphenol A with one newly-isolated strain *Bacillus* sp GZB: Kinetics, mechanism and estrogenic transition. *Bioresour. Technol.* **2012**, *114*, 224−230, DOI: 10.1016/j.biortech.2012.03.067.

(33) Pehlivanoglu, E.; Sedlak, D. L. Bioavailability of wastewater-derived organic nitrogen to the alga *Selenastrum capricornutum*. *Water Res.* **2004**, *38* (14−15), 3189−3196, DOI: 10.1016/j.watres.2004.04.027.

(34) Miao, A. J.; Wang, W. X.; Juneau, P. Comparison of Cd, Cu, and Zn toxic effects on four marine phytoplankton by pulse-amplitude-modulated fluorometry. *Environ. Toxicol. Chem.* **2005**, *24* (10), 2603−2611, DOI: 10.1897/05-009R.1.

(35) Chen, C. H.; Han, R. M.; Liang, R.; Fu, L. M.; Wang, P.; Ai, X. C.; Zhang, J. P.; Skibsted, L. H. Direct observation of the beta-carotene reaction with hydroxyl radical. *J. Phys. Chem. B* **2011**, *115* (9), 2082−2089, DOI: 10.1021/jp1100889.

(36) Mezyk, S. P.; Jones, J.; Cooper, W. J.; Tobien, T.; Nickelsen, M. G.; Adams, J. W.; O'Shea, K. E.; Bartels, D. M.; Wishart, J. F.; Tornatore, P. M.; Newman, K. S.; Gregoire, K.; Weidman, D. J. Radiation chemistry of methyl tert-butyl ether in aqueous solution. *Environ. Sci. Technol.* **2004**, *38* (14), 3994−4001, DOI: 10.1021/es034558t.

(37) Gadosy, T. A.; Shukla, D.; Johnston, L. J. Generation, characterization, and deprotonation of phenol radical cations. *J. Phys. Chem. A* **1999**, *103* (44), 8834−8839, DOI: 10.1021/jp992216x.

(38) Land, E. J.; Ebert, M. Pulse Radiolysis Studies of Aqueous Phenol - Water elimination from dihydroxycyclohexadienyl radicals to form phenoxyl. *Trans. Faraday Soc.* **1967**, *63* (533P), 1181−1190, DOI: 10.1039/tf9676301181.

(39) Swoboda, F.; Solar, S. Comparative study on the radiolytic degradation of 4-hydroxybenzoate and 4-hydroxybenzoic ethyl ester. *Radiat. Phys. Chem.* **1999**, *56* (3), 291−301, DOI: 10.1016/S0969-806X(98)00350-8.

(40) Teel, A. L.; Warberg, C. R.; Atkinson, D. A.; Watts, R. J. Comparison of mineral and soluble iron Fenton's catalysts for the treatment of trichloroethylene. *Water Res.* **2001**, *35* (4), 977−984, DOI: 10.1016/S0043-1354(00)00332-8.

(41) El-Morsi, T. M.; Budakowski, W. R.; Abd-El-Aziz, A. S.; Friesen, K. J. Photocatalytic degradation of 1,10-dichlorodecane in aqueous suspensions of TiO_2: A reaction of adsorbed chlorinated alkane with surface hydroxyl radicals. *Environ. Sci. Technol.* **2000**, *34* (6), 1018−1022, DOI: 10.1021/es9907360.

(42) Minero, C.; Mariella, G.; Maurino, V.; Vione, D.; Pelizzetti, E. Photocatalytic transformation of organic compounds in the presence of inorganic ions. 2. Competitive reactions of phenol and alcohols an a titanium dioxide-fluoride system. *Langmuir* **2000**, *16* (23), 8964−8972, DOI: 10.1021/la0005863.

(43) Chen, Y. X.; Yang, S. Y.; Wang, K.; Lou, L. P. Role of primary active species and TiO_2 surface characteristic in UV-illuminated photodegradation of Acid Orange 7. *J. Photochem. Photobiol., A* **2005**, *172* (1), 47−54, DOI: 10.1016/j.jphotochem.2004.11.006.

(44) Muneer, M.; Bahnemann, D.; Qamar, M.; Tariq, M. A.; Faisal, M. Photocatalysed reaction of few selected organic systems in presence

of titanium dioxide. *Appl. Catal., A* **2005**, *289* (2), 224−230, DOI: 10.1016/j.apcata.2005.05.003.
(45) Giraldo, A. L.; Peñuela, G. A.; Torres-Palma, R. A.; Pino, N. J.; Palominos, R. A.; Mansilla, H. D. Degradation of the antibiotic oxolinic acid by photocatalysis with TiO_2 in suspension. *Water Res.* **2010**, *44* (18), 5158−5167, DOI: 10.1016/j.watres.2010.05.011.
(46) Cho, M.; Chung, H.; Choi, W.; Yoon, J. Linear correlation between inactivation of *E. coli* and OH radical concentration in TiO_2 photocatalytic disinfection. *Water Res.* **2004**, *38* (4), 1069−1077, DOI: 10.1016/j.watres.2003.10.029.
(47) Zhang, L. S.; Wong, K. H.; Yip, H. Y.; Hu, C.; Yu, J. C.; Chan, C. Y.; Wong, P. K. Effective photocatalytic disinfection of *E. coli* K-12 using AgBr-Ag-Bi_2WO_6 nanojunction system irradiated by visible light: The role of diffusing hydroxyl radicals. *Environ. Sci. Technol.* **2010**, *44* (4), 1392−1398, DOI: 10.1021/es903087w.
(48) Poulain, L.; Monod, A.; Wortham, H. Development of a new on-line mass spectrometer to study the reactivity of soluble organic compounds in the aqueous phase under tropospheric conditions: Application to OH-oxidation of N-methylpyrrolidone. *J. Photochem. Photobiol., A* **2007**, *187* (1), 10−23, DOI: 10.1016/j.jphotochem.2006.09.006.
(49) Kim, D. K.; O'Shea, K. E.; Cooper, W. J. Oxidative degradation of alternative gasoline oxygenates in aqueous solution by ultrasonic irradiation: Mechanistic study. *Sci. Total Environ.* **2012**, *430*, 246−259, DOI: 10.1016/j.scitotenv.2011.09.016.
(50) Howard, J. A.; Ingold, K. U. Self-reaction of *sec*-butylperoxy radicals. Confirmation of Russell mechanism. *J. Am. Chem. Soc.* **1968**, *90* (4), 1056−1058, DOI: 10.1021/ja01006a037.
(51) Russell, G. A. Deuterium-isotope effects in the autoxidation of aralkyl hydrocarbons - Mechanism of the interaction of peroxy radicals. *J. Am. Chem. Soc.* **1957**, *79* (14), 3871−3877, DOI: 10.1021/ja01571a068.
(52) Bennett, J. E.; Summers, R. Product studies of mutual termination reactions of *sec*-alkylperoxy radicals - Evidence for non-cyclic termination. *Can. J. Chem.* **1974**, *52* (8), 1377−1379, DOI: 10.1139/v74-209.
(53) Schultis, T.; Metzger, J. W. Determination of estrogenic activity by LYES-assay (yeast estrogen screen-assay assisted by enzymatic digestion with lyticase). *Chemosphere* **2004**, *57* (11), 1649−1655, DOI: 10.1016/j.chemosphere.2004.06.027.
(54) Zona, R.; Solar, S. Oxidation of 2,4-dichlorophenoxyacetic acid by ionizing radiation: Degradation, detoxification and mineralization. *Radiat. Phys. Chem.* **2003**, *66* (2), 137−143, DOI: 10.1016/S0969-806X(02)00330-4.
(55) Mendez-Arriaga, F.; Esplugas, S.; Gimenez, J. Photocatalytic degradation of non-steroidal anti-inflammatory drugs with TiO_2 and simulated solar irradiation. *Water Res.* **2008**, *42* (3), 585−594, DOI: 10.1016/j.watres.2007.08.002.